frontiers in Applied Mathematics and Statistics

ORIGINAL RESEARCH
published: 17 March 2022
doi: 10.3389/fams.2022.830530

Instantaneous Frequency-Embedded Synchrosqueezing Transform for Signal Separation

Qingtang Jiang[1]*, *Ashley Prater-Bennette*[2], *Bruce W. Suter*[3] and *Abdelbaset Zeyani*[4]

[1] Department of Mathematics and Statistics, University of Missouri–St. Louis, St. Louis, MO, United States, [2] The Air Force Research Laboratory, AFRL/RISB, Rome, NY, United States, [3] The Air Force Research Laboratory, AFRL, Rome, NY, United States, [4] Department of Mathematics, Wichita State University, Wichita, KS, United States

The synchrosqueezing transform (SST) and its variants have been developed recently as an alternative to the empirical mode decomposition scheme to model a non-stationary signal as a superposition of amplitude- and frequency-modulated Fourier-like oscillatory modes. In particular, SST performs very well in estimating instantaneous frequencies (IFs) and separating the components of non-stationary multicomponent signals with slowly changing frequencies. However its performance is not desirable for signals having fast-changing frequencies. Two approaches have been proposed for this issue. One is to use the 2nd-order or high-order SST, and the other is to apply the instantaneous frequency-embedded SST (IFE-SST). For the SST or high order SST approach, one single phase transformation is applied to estimate the IFs of all components of a signal, which may yield not very accurate results in IF estimation and component recovery. IFE-SST uses an estimation of the IF of a targeted component to produce accurate IF estimation. The phase transformation of IFE-SST is associated with the targeted component. Hence the IFE-SST has certain advantages over SST in IF estimation and signal separation. In this article, we provide theoretical study on the instantaneous frequency-embedded short-time Fourier transform (IFE-STFT) and the associated SST, called IFE-FSST. We establish reconstructing properties of IFE-STFT with integrals involving the frequency variable only and provide reconstruction formula for individual components. We also consider the 2nd-order IFE-FSST.

Keywords: short-time Fourier transform, synchrosqueezing transform, instantaneous frequency-embedded STFT, instantaneous frequency-embedded SST, instantaneous frequency estimation

AMS Mathematics Subject Classification: 42C15, 42A38

OPEN ACCESS

Edited by:
Hau-Tieng Wu,
Duke University, United States

Reviewed by:
Duong Hung Pham,
UMR5505 Institut de Recherche en Informatique de Toulouse (IRIT), France
Anouar Ben Mabrouk,
University of Kairouan, Tunisia

****Correspondence:***
Qingtang Jiang
jiangq@umsl.edu

Specialty section:
This article was submitted to Mathematics of Computation and Data Science, a section of the journal Frontiers in Applied Mathematics and Statistics

Received: *07 December 2021*
Accepted: *17 February 2022*
Published: *17 March 2022*

Citation:
Jiang Q, Prater-Bennette A, Suter BW and Zeyani A (2022) Instantaneous Frequency-Embedded Synchrosqueezing Transform for Signal Separation. Front. Appl. Math. Stat. 8:830530. doi: 10.3389/fams.2022.830530

1. INTRODUCTION

Recently the continuous wavelet transform-based synchrosqueezed transform (WSST) was developed in [1] as an empirical mode decomposition (EMD)-like tool to model a non-stationary signal $x(t)$ as

$$x(t) = A_0(t) + \sum_{k=1}^{K} x_k(t), \qquad x_k(t) = A_k(t)e^{i2\pi\phi_k(t)}, \tag{1}$$

with $A_k(t), \phi_k'(t) > 0$, where $A_k(t)$ is called the instantaneous amplitudes and $\phi_k'(t)$ the instantaneous frequencies (IFs). The representation (1) of non-stationary signals is important to extract information hidden in $x(t)$. WSST not only sharpens the time-frequency representation of a signal, but also recovers the components of a multicomponent signal. The synchrosqueezing transform (SST) provides an alternative to the EMD method introduced in [2] and its variants considered in many articles such as [3–12], and it overcomes some limitations of the EMD and ensemble EMD schemes such as mode-mixing. Many works on SST have been carried out since the publication of the seminal article [1]. For example, the short-time Fourier transform (STFT)-based SST (FSST) [13–15], the 2nd-order SST [16–18], the higher-order FSST [19, 20], a hybrid EMD-WSST [21], the WSST with vanishing moment wavelets [22], the multitapered SST [23], the synchrosqueezed wave packet transform [24] and the synchrosqueezed curvelet transform [25] were proposed. Furthermore, the adaptive SST with a window function having a changing parameter was proposed in [26–31]. SST has been successfully used in machine fault diagnosis [32, 33], and medical data analysis applications [see [34] and references therein]. [35] proposed a direct time-frequency method (called SSO) based on the ridges of spectrogram for signal separation. This method has been extended recently to the linear chirp-based models [36, 37] and the models based on the CWT scaleogram [38, 39]. A hybrid EMD-SSO computational scheme was developed in [40].

If the IFs $\phi_k'(t)$ of the components $x_k(t)$ of a non-stationary multicomponent signal change slowly or change slowly compared with $\phi_k(t)$, then SST performs very well in estimating $\phi_k'(t)$ and separating the components $x_k(t)$ from $x(t)$. However its performance is not desirable for signals having fast-changing frequencies. The 2nd-order and high-order SSTs were proposed for this issue and they do improve the accuracy of IF estimation and component recovery. The problem with the 2nd-order and high-order SSTs is that, like the convectional SST, one single phase transformation is applied to estimate the IFs of all components of a signal, which may not yield desirable results in IF estimation or component recovery.

Another approach is to demodulate the original signal to change a wide-band component into a narrow-band component. Li and Liang [41] and Meignen et al. [42] demodulate the original signal into a pure carrier signal and apply WSST and the 2nd-order FSST to the demodulated signal, respectively. FSST based on another demodulation was proposed in [43]. The demodulation introduced in [43] transforms a one-dimensional signal, as a function of time only, into a two-dimensional bivariate function of time and time-shift. The STFT of the demodulated signal has more concentrated time-frequency representation than the conventional STFT, and in the meantime it well characterizes time-frequency properties of the signal [43]. The demodulation approach of [43] is considered in [44] in the setting of CWT. The associated CWT and SST are called in [44] the instantaneous frequency-embedded CWT (IFE-CWT) and IFE-SST, respectively. For consistency, we call the STFT of the demodulated signal and the associated FSST in [43]: the IFE-STFT and IFE-FSST respectively. [43] shows that IFE-FSST results in sharp time-frequency representations of signals. However component recovery of a multicomponent signal was not discussed in [43]. In this article, we consider theoretical analysis of IFE-STFT for establishing the component recovery with IFE-FSST. Compared with the study of IFE-SST in [44], we derive in this article mathematically rigorous phase transformation for IFE-FSST. In addition, in this article we also consider the 2nd-order IFE-FSST and derive the associate phase transformation.

The rest of this article is organized as follows. In Section 2, we briefly review FSST and the 2nd-order FSST. After that, we consider in Section 3 the IFE-STFT and establish reconstructing properties of IFE-STFT with integrals involving the frequency variable only. In Section 4, we derive mathematically rigorous phase transformations for IFE-FSST and the 2nd-order IFE-FSST. In addition, we provide reconstruction formula for individual components. Implementations and IFE-FSST-based component recovery algorithms are discussed in Section 5. Some experimental results are also provided in Section 5.

2. SHORT-TIME FOURIER TRANSFORM-BASED SST

The (modified) short-time Fourier transform (STFT) of $x(t)$ is defined by

$$V_x(t,\eta) := \int_{-\infty}^{\infty} x(\tau)g(\tau-t)e^{-i2\pi\eta(\tau-t)}d\tau, \tag{2}$$

where $g(t)$ is a window function with $g(0) \neq 0$. $x(t)$ can be reconstructed from its STFT:

$$x(t) = \frac{1}{\|g\|_2^2}\int_{-\infty}^{\infty}\int_{-\infty}^{\infty} V_x(t,\xi)\overline{g(t-\tau)}e^{-i2\pi\xi(\tau-t)}d\tau\, d\xi. \tag{3}$$

$x(t)$ can also be recovered back from its STFT with an integral involving only the frequency variable η:

$$x(t) = \frac{1}{g(0)}\int_{-\infty}^{\infty} V_x(t,\eta)d\eta. \tag{4}$$

In addition, one can show that if $g(t)$ and $x(t)$ are real-valued, then

$$x(t) = \frac{2}{g(0)}\mathrm{Re}\Big(\int_{0}^{\infty} V_x(t,\eta)d\eta\Big). \tag{5}$$

Furthermore, one can verify that STFT can be written as

$$V_x(t,\eta) = \int_{-\infty}^{\infty} \widehat{x}(\xi)\widehat{g}(\eta-\xi)e^{i2\pi t\xi}d\xi. \tag{6}$$

The STFT $V_x(t,\eta)$ of a slowly growing $x(t)$ is well-defined and the above formulas still hold if the window function $g(t)$ has certain smoothness and certain decaying order as $t \to \infty$, for example $g(t)$ is in the Schwarz class $\mathcal{S}$. In this article, unless otherwise stated, we always assume that a window function $g(t)$ has certain smoothness and decaying properties and $g(0) \neq 0$, and assume that a signal $x(t)$ is a slowly growing function.

2.1. FSST

The idea of FSST is to re-assign the frequency variable η of $V_x(t,\eta)$. First we look at the STFT of $x(t) = Ae^{i2\pi\xi_0 t}$, where ξ_0 is a positive constant. With

$$\begin{aligned} V_x(t,\eta) &= \int_{-\infty}^{\infty} Ae^{i2\pi\xi_0\tau} g(\tau - t)e^{-i2\pi\eta(\tau-t)}d\tau \\ &= A\widehat{g}(\eta - \xi_0)e^{i2\pi t\xi_0}, \end{aligned}$$

we can obtain the IF ξ_0 of $x(t)$ by

$$\frac{\partial_t V_x(t,\eta)}{2\pi i V_x(t,\eta)} = \xi_0,$$

where throughout this article, ∂_t denotes the partial derivative with respect to variable t. For a general $x(t)$, at (t,η) for which $V_x(t,\eta) \neq 0$, a good candidate for the IF of $x(t)$ is

$$\frac{\partial_t V_x(t,\eta)}{2\pi i V_x(t,\eta)}.$$

In the following, denote

$$\omega_x(t,\eta) := \mathrm{Re}\Big\{\frac{\partial_t V_x(t,\eta)}{2\pi i V_x(t,\eta)}\Big\}, \quad \text{for } (t,\eta) \text{ with } V_x(t,\eta) \neq 0,$$

which is called the "phase transformation" [1], "instantaneous frequency information" [13], or the "reference IF function" in [21]. FSST is to re-assign the frequency variable η by transforming the STFT $V_x(t,\eta)$ of $x(t)$ to a quantity, denoted by $R_x^{\lambda,\gamma}(t,\xi)$, on the time-frequency plane defined by

$$R_x^{\lambda,\gamma}(t,\xi) := \int_{\{\eta : |V_x(t,\eta)|>\gamma\}} V_x(t,\eta)\frac{1}{\lambda}h\left(\frac{\xi - \omega_x(t,\eta)}{\lambda}\right)d\eta,$$

where ξ is the frequency variable, $h(t)$ a compactly supported function with certain smoothness and $\int_{-\infty}^{\infty} h(t)dt = 1$, $\gamma > 0$ is the threshold for zero and $\lambda > 0$ is a dilation. As $\lambda, \gamma \to 0$, FSST is rewritten as

$$R_x(t,\xi) := \int_{\{\eta : V_x(t,\eta)\neq 0\}} V_x(t,\eta)\delta\big(\omega_x(t,\eta) - \xi\big)d\eta. \tag{7}$$

For simplicity of presentation, throughout this article SSTs will be expressed as (7).

Due to (4), we have that the input signal $x(t)$ can be recovered from its FSST by

$$x(t) = \frac{1}{g(0)}\int_{-\infty}^{\infty} R_x(t,\xi)d\xi. \tag{8}$$

If in addition, $g(t)$ and $x(t)$ are real-valued, then by (5),

$$x(t) = \frac{2}{g(0)}\mathrm{Re}\Big(\int_0^{\infty} R_x(t,\xi)d\xi\Big). \tag{9}$$

For a multicomponent signal $x(t)$ given by (1), when $A_k(t), \phi_k(t)$ satisfy certain conditions, each component $x_k(t)$ can be recovered from its FSST:

$$x_k(t) \approx \frac{1}{g(0)}\int_{|\xi - \mathrm{IF}_k(t)|<\Gamma} R_x(t,\xi)d\xi, \tag{10}$$

for certain $\Gamma > 0$, where $\mathrm{IF}_k(t)$ is an estimate to $\phi_k'(t)$. See [13–15] for the details.

In practice, t, η, ξ are discretized. Suppose t_n, η_j, ξ_m are the sampling points of t, η, ξ respectively. Then the FSST of $x(t)$ is given by

$$R_x(t_n,\xi_m) = \sum_{j:\ |\omega_x(t_n,\eta_j)-\xi_m|\leq\Delta\xi/2, |V_x(t_n,\eta_j)|\geq\gamma} V_x(t_n,\eta_j)\triangle\eta_j,$$

where $\triangle\eta_j = \eta_j - \eta_{j-1}$, and $\gamma > 0$ is a threshold for the condition $|V_x(t,\eta)| > 0$. The recovering formulas (8) and (9) result in

$$x(t_n) = \frac{1}{g(0)}\sum_m R_x(t_n,\xi_m)\triangle\xi_m,$$

and for real-valued $g(t)$ and $x(t)$,

$$x(t_n) = \frac{2}{g(0)}\mathrm{Re}\Big(\sum_m R_x(t_n,\xi_m)\triangle\xi_m\Big),$$

where $\triangle\xi_m = \xi_m - \xi_{m-1}$.

2.2. Second-Order FSST

The 2nd-order FSST was introduced in [16]. The main idea is to define a new phase transformation $\omega_x^{2\mathrm{nd}}$ such that when $x(t)$ is a linear frequency modulation (LFM) signal (also called a linear chirp), then $\omega_x^{2\mathrm{nd}}$ is exactly the IF of $x(t)$. We say $x(t)$ is a LFM signal or a linear chirp if

$$x(t) = Ae^{i2\pi\phi(t)} = Ae^{i2\pi(ct+\frac{1}{2}rt^2)} \tag{11}$$

with phase function $\phi(t) = ct + \frac{1}{2}rt^2$, IF $\phi'(t) = c + rt$ and chirp rate $\phi''(t) = r$. In [16], the reassignment operators are used to derive $\omega_x^{2\mathrm{nd}}$. Different phase transformation $\omega_x^{2\mathrm{nd}}$ for the 2nd-order SST can be derived without using the reassignment operators see [28, 29].

Let g be a given window function. Denote

$$g_1(t) = tg(t). \tag{12}$$

Recall that $V_x(t,\eta)$ denotes the STFT of $x(t)$ with g defined by (2). In this article, we let $V_x^{g_1}(t,\eta)$ denote the STFT of $x(t)$ with $g_1(t)$, namely, the integral on the right-hand side of (2) with $g(t)$ replaced by $g_1(t)$. Define

$$\omega_x^{2\mathrm{nd}}(t,\eta) := \begin{cases} \mathrm{Re}\Big\{\frac{\partial_t V_x(t,\eta)}{i2\pi V_x(t,\eta)}\Big\} - \mathrm{Re}\Big\{q_0(t,\eta)\frac{V_x^{g_1}(t,\eta)}{i2\pi V_x(t,\eta)}\Big\}, \\ \quad \text{if } \partial_\eta\Big(\frac{V_x^{g_1}(t,\eta)}{V_x(t,\eta)}\Big) \neq 0, V_x(t,\eta) \neq 0, \\ \mathrm{Re}\Big\{\frac{\partial_t V_x(t,\eta)}{i2\pi V_x(t,\eta)}\Big\}, \\ \quad \text{if } \partial_\eta\Big(\frac{V_x^{g_1}(t,\eta)}{V_x(t,\eta)}\Big) = 0, V_x(t,\eta) \neq 0, \end{cases} \tag{13}$$

where

$$q_0(t,\eta) := \frac{1}{\partial_\eta\Big(\frac{V_x^{g_1}(t,\eta)}{V_x(t,\eta)}\Big)}\partial_\eta\Big(\frac{\partial_t V_x(t,\eta)}{V_x(t,\eta)}\Big).$$

Then one can show that $\omega_x^{2\mathrm{nd}}(t,\eta)$ is exactly the IF $\phi'(t)$ of $x(t)$ if $x(t)$ is an LFM signal given by (11), see [19, 28]. Thus, we may define $\omega_x^{2nd}(t,\eta)$ in (13) as the phase transformation for the 2nd-order FSST. Very recently a simple phase transformation for the 2nd-order FSST was proposed in [18].

3. INSTANTANEOUS FREQUENCY-EMBEDDED STFT

IFE-FSST is based on the IFE-STFT, which is defined below.

Definition 1. *Suppose $\varphi(t)$ is a differentiable function with $\varphi'(t) > 0$. Let $\eta_0 > 0$. The IFE-STFT of $x(t) \in L_2(\mathbb{R})$ with $\varphi(t), \eta_0$ and a window function $g(t)$ is defined by*

$$V_x^{\mathrm{I}}(t,\eta) := \int_{-\infty}^{\infty} x(\tau) e^{-i2\pi\left(\varphi(\tau)-\varphi(t)-\varphi'(t)(\tau-t)-\eta_0\tau\right)} g(\tau-t) e^{-i2\pi\eta(\tau-t)} d\tau. \tag{14}$$

In the above definition, we assume $x(t) \in L_2(\mathbb{R})$. The definition of IFE-STFT can be extended to slowly growing functions $x(t)$ if $g(t)$ has certain smoothness and certain decaying order as $t \to \infty$.

Li and Liang [41] proposed the modulation $x(\tau) \to \widetilde{x}(\tau) = x(\tau)e^{-i2\pi(\varphi(\tau)-\eta_0\tau)}$ and applied WSST to the modulated signal $\widetilde{x}(\tau)$, while [42] applied the 2nd-order FSST to $\widetilde{x}(t)$. The modulation:

$$x(\tau) \to x(\tau) e^{-i2\pi\left(\varphi(\tau)-\varphi(t)-\varphi'(t)(\tau-t)-\eta_0\tau\right)}$$

introduced in [43] for IFE-FSST and also used in [44] for IFE-WSST is different from that used in [41, 42]. IFE-STFT and IFE-CWT with such a modulation not only have more concentrated time-frequency representation than the conventional STFT and CWT respectively, but also well keep the IF of the signal. The reader is referred to [43] and [44] for detailed discussions.

[43] provides a reconstruction formula with IFE-STFT for the whole signal $x(t)$, which is similar to (3) and involves an integral with both the time and frequency variables. [43] does not consider individual component recovery formula with IFE-FSST. In this article, we provide such a component recovery formula. To this regard, in this section we establish a reconstruction formula with IFE-STFT like (4), which involves an integral with the frequency variable only. First we have the following property about the IFE-STFT.

Proposition 1. *Let $V_x^{\mathrm{I}}(t,\eta)$ be the IFE-STFT of $x(t)$ defined by (14). Then*

$$V_x^{\mathrm{I}}(t,\eta) = e^{i2\pi\varphi(t)} \int_{-\infty}^{\infty} \widehat{\widetilde{x}}(\xi)\widehat{g}(\eta-\varphi'(t)-\xi)e^{i2\pi t\xi} d\xi, \tag{15}$$

where

$$\widetilde{x}(t) = x(t)e^{-i2\pi(\varphi(t)-\eta_0 t)}. \tag{16}$$

Proof: We have

$$\begin{aligned} V_x^{\mathrm{I}}(t,\eta) &= e^{i2\pi\varphi(t)} \int_{-\infty}^{\infty} \widetilde{x}(\tau) e^{i2\pi\varphi'(t)(\tau-t)} g(\tau-t) e^{-i2\pi\eta(\tau-t)} d\tau \\ &= e^{i2\pi\varphi(t)} \int_{-\infty}^{\infty} \widetilde{x}(\tau) g(\tau-t) e^{-i2\pi\left(\eta-\varphi'(t)\right)(\tau-t)} d\tau \\ &= e^{i2\pi\varphi(t)} \int_{-\infty}^{\infty} \widehat{\widetilde{x}}(\xi)\widehat{g}\big(\eta-\varphi'(t)-\xi\big) e^{i2\pi t\xi} d\xi, \end{aligned}$$

where the last equality follows from (6). □

The next theorem shows that $x(t)$ can be recovered from its IFE-STFT with an integral involving η only.

Theorem 1. *Let $x(t)$ be a function in $L_2(\mathbb{R})$. Then*

$$x(t) = \frac{e^{-i2\pi\eta_0 t}}{g(0)} \int_{-\infty}^{\infty} V_x^{\mathrm{I}}(t,\eta) d\eta. \tag{17}$$

Proof: Let $\widetilde{x}(t)$ be the function defined by (16). From (15), we have

$$\begin{aligned} \int_{-\infty}^{\infty} V_x^{\mathrm{I}}(t,\eta) d\eta &= e^{i2\pi\varphi(t)} \int_{-\infty}^{\infty}\int_{-\infty}^{\infty} \widehat{\widetilde{x}}(\xi)\widehat{g}(\eta-\varphi'(t)-\xi)e^{i2\pi t\xi} d\xi d\eta \\ &= e^{i2\pi\varphi(t)} \int_{-\infty}^{\infty} \widehat{\widetilde{x}}(\xi) \int_{-\infty}^{\infty} \widehat{g}(\eta-\varphi'(t)-\xi) d\eta\, e^{i2\pi t\xi} d\xi \\ &= e^{i2\pi\varphi(t)} g(0) \int_{-\infty}^{\infty} \widehat{\widetilde{x}}(\xi) e^{i2\pi t\xi} d\xi \\ &= e^{i2\pi\varphi(t)} g(0)\widetilde{x}(t) \\ &= e^{i2\pi\varphi(t)} g(0)x(t)e^{-i2\pi\left(\varphi(t)-\eta_0 t\right)} \\ &= g(0)x(t)e^{i2\pi\eta_0 t}. \end{aligned}$$

Thus, Equation (17) holds. □

If one is interested in $V_x^{\mathrm{I}}(t,\eta)$ with the positive frequency $\eta > 0$ only, then we have the following result on how to recover $x(t)$ from $V_x^{\mathrm{I}}(t,\eta)$.

Theorem 2. *Suppose $supp(\widehat{g}) \subseteq [-\Delta, \Delta]$ for some Δ, and $\varphi'(t) \geq \Delta$. Let $y(t) = x(t)e^{-i2\pi\varphi(t)}$. If $\widehat{y}(\eta) = 0$, $\eta \leq B$ for some constant B, then for any $\eta_0 \geq -B$,*

$$x(t) = \frac{e^{-i2\pi\eta_0 t}}{g(0)} \int_{0}^{\infty} V_x^{\mathrm{I}}(t,\eta) d\eta. \tag{18}$$

Proof: Let $\widetilde{x}(t)$ be the function defined by (16). Then $\widetilde{x}(t) = y(t)e^{i2\pi\eta_0 t}$. Thus, $\widehat{\widetilde{x}}(\xi) = \widehat{y}(\xi-\eta_0)$. Therefore, from (15), we have

$$\begin{aligned} \int_{0}^{\infty} V_x^{\mathrm{I}}(t,\eta) d\eta &= e^{i2\pi\varphi(t)} \int_{0}^{\infty}\int_{-\infty}^{\infty} \widehat{\widetilde{x}}(\xi)\widehat{g}(\eta-\varphi'(t)-\xi)e^{i2\pi t\xi} d\xi d\eta \\ &= e^{i2\pi\varphi(t)} \int_{0}^{\infty}\int_{-\infty}^{\infty} \widehat{y}(\xi-\eta_0)\widehat{g}(\eta-\varphi'(t)-\xi)e^{i2\pi t\xi} d\xi d\eta \\ &= e^{i2\pi\varphi(t)} \int_{0}^{\infty}\int_{-\infty}^{\infty} \widehat{y}(\xi)\widehat{g}(\eta-\varphi'(t)-\xi-\eta_0)e^{i2\pi t(\xi+\eta_0)} d\xi d\eta \\ &= e^{i2\pi\left(\varphi(t)+t\eta_0\right)} \int_{-\infty}^{\infty} \widehat{y}(\xi) \int_{0}^{\infty} \widehat{g}(\eta-\varphi'(t)-\xi-\eta_0)e^{i2\pi t\xi} d\eta d\xi \\ &= e^{i2\pi\left(\varphi(t)+t\eta_0\right)} \int_{B}^{\infty} \widehat{y}(\xi)e^{i2\pi t\xi} \int_{0}^{\infty} \widehat{g}(\eta-\varphi'(t)-\xi-\eta_0) d\eta d\xi. \end{aligned}$$

When $\xi \geq B$ and $\eta_0 \geq -B$, we have $-\varphi'(t) - \xi - \eta_0 \leq -\Delta - B + B = -\Delta$. This and the assumption $\mathrm{supp}(\widehat{g}) \subseteq [-\Delta, \Delta]$ lead to

$$\int_0^\infty \widehat{g}(\eta - \varphi'(t) - \xi - \eta_0)d\eta = \int_{-\varphi'(t)-\xi-\eta_0}^{\infty} \widehat{g}(\eta)d\eta = \int_{-\infty}^{\infty} \widehat{g}(\eta)d\eta = g(0).$$

Hence,

$$\begin{aligned}\int_0^\infty V_x^{\mathrm{I}}(t,\eta)d\eta &= e^{i2\pi\left(\varphi(t)+t\eta_0\right)} \int_B^\infty \widehat{y}(\xi)e^{i2\pi t\xi} g(0)d\xi \\ &= e^{i2\pi\left(\varphi(t)+t\eta_0\right)} g(0) \int_{-\infty}^\infty \widehat{y}(\xi)e^{i2\pi t\xi}d\xi \\ &= e^{i2\pi\left(\varphi(t)+t\eta_0\right)} g(0)y(t) \\ &= e^{i2\pi\left(\varphi(t)+t\eta_0\right)} g(0)x(t)e^{-i2\pi\varphi(t)} \\ &= g(0)x(t)e^{i2\pi\eta_0 t}.\end{aligned}$$

Thus, Equation (18) holds. □

Next theorem shows that when the condition $\widehat{y}(\eta) = 0, \eta \leq B$ in Theorem 2 does not hold, the integral in the right-hand side of (18) can still approximate $x(t)$ well if η_0 is large.

Theorem 3. *Let $y(t) = x(t)e^{-i2\pi\varphi(t)}$. Then*

$$x(t) = \frac{e^{-i2\pi\eta_0 t}}{g(0)} \int_0^\infty V_x^{\mathrm{I}}(t,\eta)d\eta + \mathrm{Err}, \tag{19}$$

with

$$|\mathrm{Err}| \leq \frac{\int_{-\infty}^{\infty} |\widehat{g}(\xi)|d\xi}{g(0)} \int_{-\infty}^{-\eta_0} |\widehat{y}(\xi)|d\xi.$$

Proof: By Theorem 1,

$$\begin{aligned}\int_0^\infty V_x^{\mathrm{I}}(t,\eta)d\eta &= \int_{-\infty}^\infty V_x^{\mathrm{I}}(t,\eta)d\eta - \int_{-\infty}^0 V_x^{\mathrm{I}}(t,\eta)d\eta \\ &= e^{i2\pi\eta_0 t}g(0)x(t) - \int_{-\infty}^0 V_x^{\mathrm{I}}(t,\eta)d\eta.\end{aligned}$$

Thus,

$$\mathrm{Err} = \frac{e^{-i2\pi\eta_0 t}}{g(0)} \int_{-\infty}^0 V_x^{\mathrm{I}}(t,\eta)d\eta.$$

With

$$\begin{aligned}\left|\int_{-\infty}^0 V_x^{\mathrm{I}}(t,\eta)d\eta\right| &= \left|e^{i2\pi\varphi(t)}\int_{-\infty}^0\int_{-\infty}^\infty \widehat{y}(\xi-\eta_0)\widehat{g}(\eta-\varphi'(t)-\xi)e^{i2\pi t\xi}d\xi d\eta\right| \\ &\leq \int_{-\infty}^0\int_{-\infty}^\infty |\widehat{y}(\xi-\eta_0)|\,|\widehat{g}(\eta-\varphi'(t)-\xi)e^{i2\pi t\xi}|d\eta d\xi \\ &\leq \int_{-\infty}^0 |\widehat{y}(\xi-\eta_0)| \int_{-\infty}^\infty |\widehat{g}(\eta-\varphi'(t)-\xi)|d\eta d\xi \\ &= \int_{-\infty}^\infty |\widehat{g}(\eta)|d\eta \int_{-\infty}^0 |\widehat{y}(\xi-\eta_0)|d\xi \\ &= \int_{-\infty}^\infty |\widehat{g}(\eta)|d\eta \int_{-\infty}^{-\eta_0} |\widehat{y}(\xi)|d\xi,\end{aligned}$$

we conclude that (19) holds. □

4. IFE-STFT BASED SYNCHROSQUEEZING TRANSFORM

In this section, we consider IFE-FSST, the synchrosqueezing transform based on IFE-STFT. First we show how to derive the phase transformation associated with (the 1st-order) IFE-FSST. After that we introduce the 2nd-order IFE-FSST.

4.1. IFE-FSST

To define IFE-FSST, first we need to define the corresponding phase transformation $\omega_x^{\mathrm{I}}(a,b)$. Let us consider the case $x(t) = Ae^{i2\pi\xi_0 t}$ for some $\xi_0 > 0$. With $x'(t) = i2\pi\xi_0\, x(t)$, we have

$$V_{x'}^{\mathrm{I}}(t,\eta) = i2\pi\xi_0 V_x^{\mathrm{I}}(t,\eta).$$

On the other hand,

$$\begin{aligned}V_{x'}^{\mathrm{I}}(t,\eta) &= \int_{-\infty}^\infty \partial_\tau\big(x(t+\tau)\big)e^{-i2\pi\left(\varphi(t+\tau)-\varphi(t)-\varphi'(t)\tau-\eta_0(t+\tau)\right)}g(\tau)e^{-i2\pi\eta\tau}d\tau \\ &= -\int_{-\infty}^\infty x(t+\tau)\partial_\tau\left(e^{-i2\pi\left(\varphi(t+\tau)-\varphi(t)-\varphi'(t)\tau-\eta_0(t+\tau)\right)}g(\tau)e^{-i2\pi\eta\tau}\right)d\tau \\ &= -\int_{-\infty}^\infty x(t+\tau)(-i2\pi)\big(\varphi'(t+\tau)-\varphi'(t)-\eta_0+\eta\big) \\ &\quad e^{-i2\pi\left(\varphi(t+\tau)-\varphi(t)-\varphi'(t)\tau-\eta_0(t+\tau)+\eta)\right)}g(\tau)d\tau \\ &\quad -\int_{-\infty}^\infty x(t+\tau)e^{-i2\pi\left(\varphi(t+\tau)-\varphi(t)-\varphi'(t)\tau-\eta_0(t+\tau)+\eta)\right)}g'(\tau)d\tau \\ &= i2\pi V_{x\varphi'}^{\mathrm{I}}(t,\eta) + i2\pi(\eta-\varphi'(t)-\eta_0)V_x^{\mathrm{I}}(t,\eta) - V_x^{\mathrm{I},g'}(t,\eta),\end{aligned} \tag{20}$$

where $V_x^{\mathrm{I},g'}(t,\eta)$ denotes the IFE-STFT of $x(t)$ defined by (14) with $\varphi(t)$ and the window function g' given by (12). Thus, if $V_x^{\mathrm{I}}(t,\eta) \neq 0$, then

$$\xi_0 = \frac{V_{x'}^{\mathrm{I}}(t,\eta)}{i2\pi V_x^{\mathrm{I}}(t,\eta)} = \frac{i2\pi V_{x\varphi'}^{\mathrm{I}}(t,\eta) - V_x^{\mathrm{I},g'}(t,\eta)}{i2\pi V_x^{\mathrm{I}}(t,\eta)} + \eta - \varphi'(t) - \eta_0.$$

Based on the above discussion, for a general signal $x(t)$, we define the phase transformation $\omega_x^{\mathrm{I}}(a,b)$ of the IFE-FSST of $x(t)$ to be

$$\omega_x^{\mathrm{I}}(t,\eta) := \mathrm{Re}\Big(\frac{i2\pi V_{x\varphi'}^{\mathrm{I}}(t,\eta) - V_x^{\mathrm{I},g'}(t,\eta)}{i2\pi V_x^{\mathrm{I}}(t,\eta)}\Big) + \eta - \varphi'(t) - \eta_0. \tag{21}$$

Definition 2. *Suppose $\varphi(t)$ is a differentiable function with $\varphi'(t) > 0$. The IFE-FSST of a signal $x(t)$ with φ and ξ_0 is defined by*

$$R_x^{\mathrm{I}}(t,\xi) := \int_{\{\eta\,:\,V_x^{\mathrm{I}}(t,\eta)\neq 0\}} V_x^{\mathrm{I}}(t,\eta)\delta\big(\omega_x^{\mathrm{I}}(t,\eta)-\xi\big)d\eta$$

where $\omega_x^{\mathrm{I}}(t,\eta)$ is the phase transformation defined by (21).

The IFE-FSST is called the demodulation transform-based SST in [43]. The corresponding phase transformation in [43] is different from our $\omega_x^{\mathrm{I}}(t,\eta)$ defined in (21).

By (18) in Theorem 1, we know the input signal $x(t)$ can be recovered from its IFE-FSST as shown in the following:
For $x(t) \in L_2(\mathbb{R})$,

$$x(t) = \frac{e^{-i2\pi\eta_0 t}}{g(0)} \int_{-\infty}^{\infty} R_x^{\mathrm{I}}(t,\xi)d\xi; \tag{22}$$

and if, in addition, the conditions in Theorem 2 hold, then

$$x(t) = \frac{e^{-i2\pi\eta_0 t}}{g(0)} \int_{0}^{\infty} R_x^{\mathrm{I}}(t,\xi)d\xi. \tag{23}$$

For a multicomponent signal $x(t)$ in the form (1), if $R_{x_k}^{\mathrm{I}}(t,\xi)$, $1 \le k \le K$ lie in different time-frequency zones, then following (18), we know $x_k(t)$ can be recovered from its IFE-FSST:

$$x_k(t) \approx \frac{e^{-i2\pi\eta_0 t}}{g(0)} \int_{|\xi-\mathrm{IF}_k(t)|<\Gamma_1} R_x^{\mathrm{I}}(t,\xi)d\xi, \tag{24}$$

for certain $\Gamma_1 > 0$, where $\mathrm{IF}_k(t)$ is an estimate of $\phi_k'(t)$. If $x_k(t)$ and $g(t)$ are real-valued, then

$$x_k(t) \approx \frac{2}{g(0)} \mathrm{Re}\Big(e^{-i2\pi\eta_0 t} \int_{|\xi-\mathrm{IF}_k(t)|<\Gamma_1} R_x^{\mathrm{I}}(t,\xi)d\xi\Big). \tag{25}$$

4.2. 2nd-Order IFE-FSST

In this subsection, we propose the 2nd-order IFE-FSST. The key point is, based on IFE-STFT, to define a phase transformation $\omega_x^{\mathrm{I,2nd}}(t,\eta)$ which is the IF $\phi'(t)$ of $x(t)$ when $x(t)$ is a linear chirp given by (11). As above, for $g_1(t) = tg(t)$, we use $V_x^{\mathrm{I},g_1}(t,\eta)$ to denote the IFE-STFT of $x(t)$ with the window function $g_1(t)$, namely, the integral on the right-hand side of (14) with $g(t)$ replaced by $g_1(t)$. Next we define the phase transformation $\omega_x^{\mathrm{I,2nd}}(t,\eta)$ for the 2nd-order IFE-FSST to be:

$$\omega_x^{\mathrm{I,2nd}}(t,\eta) := \begin{cases} \omega_x^{\mathrm{I}}(t,\eta) - \mathrm{Re}\Big\{Q_0(t,\eta)\frac{V_x^{\mathrm{I},g_1}(t,\eta)}{i2\pi V_x^{\mathrm{I}}(t,\eta)}\Big\}, \\ \qquad \text{if } \partial_\eta\big(\frac{V_x^{\mathrm{I},g_1}(t,\eta)}{V_x^{\mathrm{I}}(t,\eta)}\big) \ne 0, V_x^{\mathrm{I}}(t,\eta) \ne 0; \\ \omega_x^{\mathrm{I}}(t,\eta), \\ \qquad \text{if } \partial_\eta\big(\frac{V_x^{\mathrm{I},g_1}(t,\eta)}{V_x^{\mathrm{I}}(t,\eta)}\big) = 0, V_x^{\mathrm{I}}(t,\eta) \ne 0, \end{cases} \tag{26}$$

where $\omega_x^{\mathrm{I}}(t,\eta)$ is defined by (21), and

$$Q_0(t,\eta) := \frac{1}{\partial_\eta\Big(\frac{V_x^{\mathrm{I},g_1}(t,\eta)}{V_x^{\mathrm{I}}(t,\eta)}\Big)} \Big\{1 + \partial_\eta\Big(\frac{i2\pi V_{x\varphi'}^{\mathrm{I}}(t,\eta) - V_x^{\mathrm{I},g'}(t,\eta)}{i2\pi V_x^{\mathrm{I}}(t,\eta)}\Big)\Big\}. \tag{27}$$

Theorem 4. *If $x(t)$ is a linear chirp signal given by (11), then at (t,η) where $V_x^{\mathrm{I}}(t,\eta) \ne 0$, $\partial_\eta\big(V_x^{\mathrm{I},g_1}(t,\eta)/V_x^{\mathrm{I}}(t,\eta)\big) \ne 0$, $\omega_x^{\mathrm{I,2nd}}(t,\eta)$ defined by (26) is the IF of $x(t)$, namely $\omega_x^{\mathrm{I,2nd}}(t,\eta) = c + rt$.*

Proof: Here, we provide the proof of $\omega_x^{\mathrm{I,2nd}}(t,\eta) = c+rt$ for more general linear chirp signals given by

$$x(t) = A(t)e^{i2\pi\phi(t)} = Ae^{pt+\frac{q}{2}t^2} e^{i2\pi(ct+\frac{1}{2}rt^2)} \tag{28}$$

where p, q are real numbers.

For the simplicity of presentation, we denote

$$M_{\varphi,g}(\tau,t,\eta) := e^{-i2\pi\big(\varphi(t+\tau)-\varphi(t)-\varphi'(t)\tau-\eta_0(t+\tau)\big)} g(\tau)e^{-i2\pi\eta\tau},$$

and thus, $V_x^{\mathrm{I}}(t,\eta)$ can simply be written as

$$V_x^{\mathrm{I}}(t,\eta) = \int_{-\infty}^{\infty} x(t+\tau)M_{\varphi,g}(\tau,t,\eta)d\tau.$$

Observe that for $x(t)$ given by (28), we have

$$x'(t) = \big(p + qt + i2\pi(c+rt)\big)x(t).$$

Thus,

$$\begin{aligned} V_{x'}^{\mathrm{I}}(t,\eta) &= \int_{-\infty}^{\infty} x'(t+\tau)\, M_{\varphi,g}(\tau,t,\eta)d\tau \\ &= \int_{-\infty}^{\infty} \big(p + q(t+\tau) + i2\pi(c+rt+r\tau)\big) \\ &\qquad x(t+\tau)\, M_{\varphi,g}(\tau,t,\eta)d\tau \\ &= \big(p+qt+i2\pi(c+rt)\big)V_x^{\mathrm{I}}(t,\eta) \\ &\quad +(q+i2\pi r)\int_{-\infty}^{\infty} x(t+\tau)\ \tau M_{\varphi,g}(\tau,t,\eta)\tau d\tau \\ &= \big(p+qt+i2\pi(c+rt)\big)V_x^{\mathrm{I}}(t,\eta) \\ &\quad +(q+i2\pi r)V_x^{\mathrm{I},g_1}(t,\eta). \end{aligned}$$

On the other hand, as shown above, $V_{x'}^{\mathrm{I}}(t,\eta)$ is equal to the quantity in (20). Therefore,

$$\begin{aligned} &\big(p+qt+i2\pi(c+rt)\big)V_x^{\mathrm{I}}(t,\eta) + (q+i2\pi r)V_x^{\mathrm{I},g_1}(t,\eta) \\ &\quad = i2\pi V_{x\varphi'}^{\mathrm{I}}(t,\eta) + i2\pi(\eta - \varphi'(t) - \eta_0)V_x^{\mathrm{I}}(t,\eta) \\ &\quad - V_x^{I,g'}(t,\eta). \end{aligned}$$

Hence, at (t,η) on which $V_x^{\mathrm{I}}(t,\eta) \ne 0$, we have

$$\begin{aligned} &\frac{p+qt}{i2\pi} + c + rt + (\frac{q}{i2\pi} + r)\frac{V_x^{\mathrm{I},g_1}(t,\eta)}{V_x^{\mathrm{I}}(t,\eta)} \\ &\quad = \frac{i2\pi V_{x\varphi'}^{\mathrm{I}}(t,\eta) - V_x^{I,g'}(t,\eta)}{i2\pi V_x^{\mathrm{I}}(t,\eta)} + \eta - \varphi'(t) - \eta_0. \end{aligned} \tag{29}$$

Taking partial derivative ∂_η to the both sides of (29), we have

$$(\frac{q}{i2\pi} + r)\partial_\eta\Big(\frac{V_x^{\mathrm{I},g_1}(t,\eta)}{V_x^{\mathrm{I}}(t,\eta)}\Big) = 1 + \partial_\eta\Big(\frac{i2\pi V_{x\varphi'}^{\mathrm{I}}(t,\eta) - V_x^{I,g'}(t,\eta)}{i2\pi V_x^{\mathrm{I}}(t,\eta)}\Big),$$

which leads to

$$\frac{q}{i2\pi} + r = Q_0(t,\eta),$$

for (t,η) with $\partial_\eta\big(V_x^{\mathrm{I},g_1}(t,\eta)/V_x^{\mathrm{I}}(t,\eta)\big) \neq 0$, where $Q_0(t,\eta)$ is defined by (27).

Returning back to (29) with $\frac{q}{i2\pi}+r$ replaced by $Q_0(t,\eta)$, we have

$$\begin{aligned} c+rt = &\frac{i2\pi V^{\mathrm{I}}_{x\varphi'}(t,\eta) - V_x^{\mathrm{I},g'}(t,\eta)}{i2\pi V^{\mathrm{I}}_x(t,\eta)} \\ &+\eta-\varphi'(t)-\eta_0-\frac{p+qt}{i2\pi} - Q_0(t,\eta)\frac{V_x^{\mathrm{I},g_1}(t,\eta)}{V_x^{\mathrm{I}}(t,\eta)}. \end{aligned}$$

Since $c+rt$ is real, taking the real parts of the quantities in the above equation, we have

$$\begin{aligned} c+rt &= \mathrm{Re}\Big\{\frac{i2\pi V^{\mathrm{I}}_{x\varphi'}(t,\eta) - V_x^{\mathrm{I},g'}(t,\eta)}{i2\pi V^{\mathrm{I}}_x(t,\eta)}\Big\} \\ &\quad +\eta-\varphi'(t)-\eta_0-\mathrm{Re}\Big\{Q_0(t,\eta)\frac{V_x^{\mathrm{I},g_1}(t,\eta)}{V_x^{\mathrm{I}}(t,\eta)}\Big\} \\ &= \omega_x^{\mathrm{I}}(t,\eta)-\mathrm{Re}\Big\{Q_0(t,\eta)\frac{V_x^{\mathrm{I},g_1}(t,\eta)}{V_x^{\mathrm{I}}(t,\eta)}\Big\}, \end{aligned}$$

which is $\omega_x^{\mathrm{I,2nd}}(t,\eta)$. This completes the proof of Theorem 4. □

With the phase transformation $\omega_x^{\mathrm{I,2nd}}(t,\eta)$ in (26), we have the corresponding 2nd-order IFE-FSST of a signal $x(t)$ with φ, ξ_0 and window function g defined by

$$R_x^{\mathrm{I},2}(t,\xi) := \int_{\{\eta:\,V_x^{\mathrm{I}}(t,\eta)\neq 0\}} V_x^{\mathrm{I}}(t,\eta)\delta\big(\omega_x^{\mathrm{I,2nd}}(t,\eta)-\xi\big)d\eta. \tag{30}$$

One has reconstruction formulas with $R_x^{\mathrm{I},2}(t,\xi)$ similar to (22)–(25).

5. IMPLEMENTATION AND EXPERIMENTAL RESULTS

5.1. Calculating $\omega_x^{\mathrm{I}}(t,\eta)$ and $\omega_x^{\mathrm{I},2nd}(t,\eta)$

First we consider the IFE-FSST. We need to calculate $\omega_x^{\mathrm{I}}(t,\eta)$. We will use (15) so that FFT can be applied to (discrete signals) x and $x\varphi'$ to calculate $V^{\mathrm{I}}(t,\eta)$, $V^{\mathrm{I}}_{x\varphi'}(t,\eta)$ and $V_x^{\mathrm{I},g'}(t,\eta)$. $V^{\mathrm{I}}_{x\varphi'}(t,\eta)$ can be obtained by (15) with x replaced by $x\varphi'$. As long as $V_x^{\mathrm{I},g'}(t,\eta)$ is concerned, observe that the Fourier transform of g' is $i2\pi\xi\,\widehat{g}(\xi)$. Hence

$$\begin{aligned} V_x^{\mathrm{I},g'}(t,\eta) = e^{i2\pi\varphi(t)}\int_{\mathbb{R}} &\widehat{x}(\xi) i2\pi(\eta-\varphi'(t)-\xi) \\ &\widehat{g}(\eta-\varphi'(t)-\xi)e^{i2\pi t\xi}d\xi. \end{aligned}$$

After obtaining $V^{\mathrm{I}}(t,\eta)$, $V^{\mathrm{I}}_{x\varphi'}(t,\eta)$ and $V_x^{\mathrm{I},g'}(t,\eta)$, we get $\omega_x^{\mathrm{I}}(t,\eta)$ and then the IFE-FSST.

For the 2nd-order IFE-FSST, we need to calculate

$$V_x^{\mathrm{I},g_1}(t,\eta),\ \partial_\eta\Big(V_x^{\mathrm{I}}(t,\eta)\Big),\ \partial_\eta\Big(V_x^{\mathrm{I},g_1}(t,\eta)\Big),\ \partial_\eta\Big(V^{\mathrm{I}}_{x\varphi'}(t,\eta)\Big),$$
$$\partial_\eta\Big(V_x^{\mathrm{I},g'}(t,\eta)\Big).$$

Note that the Fourier transform of $\tau g(\tau)$ is

$$\begin{aligned} \int_{\mathbb{R}}\tau g(\tau)e^{-i2\pi\xi\tau}d\tau &= \frac{1}{-i2\pi}\frac{d}{d\xi}\Big(\int_{\mathbb{R}} g(\tau)e^{-i2\pi\xi\tau}d\tau\Big) \\ &= \frac{1}{-i2\pi}\big(\widehat{g}\big)'(\xi). \end{aligned}$$

Thus, we conclude

$$V_x^{\mathrm{I},g_1}(t,\eta) = -e^{i2\pi\varphi(t)}\frac{1}{i2\pi}\int_{\mathbb{R}}\widehat{x}(\xi)\ \big(\widehat{g}\big)'(\eta-\varphi'(t)-\xi)e^{i2\pi t\xi}d\xi. \tag{31}$$

By the fact $\partial_\eta\Big(V_x^{\mathrm{I}}(t,\eta)\Big) = -i2\pi V_x^{\mathrm{I},g_1}(t,\eta)$, we can obtain $\partial_\eta\Big(V_x^{\mathrm{I}}(t,\eta)\Big)$ and $\partial_\eta\Big(V^{\mathrm{I}}_{x\varphi'}(t,\eta)\Big)$ as well *via* (31).

To calculate $\partial_\eta\big(V_x^{\mathrm{I},g_1}(t,\eta)\big)$, with $\partial_\eta\big(V_x^{\mathrm{I},g_1}(t,\eta)\big) = -i2\pi V_x^{\mathrm{I},g_2}(t,\eta)$, where $g_2(\tau)=\tau^2 g(\tau)$, we need to calculate the Fourier transform of $g_2(\tau)$, which is

$$\widehat{g_2}(\xi) = \frac{1}{(-i2\pi)^2}\frac{d^2}{d\xi^2}\Big(\int_{\mathbb{R}} g(\tau)e^{-i2\pi\xi\tau}d\tau\Big) = -\frac{1}{4\pi^2}\big(\widehat{g}\big)''(\xi).$$

Therefore,

$$\partial_\eta\Big(V_x^{\mathrm{I},g_1}(t,\eta)\Big) = -e^{i2\pi\varphi(t)}\frac{1}{i2\pi}\int_{\mathbb{R}}\widehat{x}(\xi)\ \big(\widehat{g}\big)''(\eta-\varphi'(t)-\xi)e^{i2\pi t\xi}d\xi. \tag{32}$$

For $\partial_\eta\Big(V_x^{\mathrm{I},g'}(t,\eta)\Big)$, we need to calculate the Fourier transform of $\tau g'(\tau)$, denoted by $\big(\tau g'(\tau)\big)^\wedge(\xi)$. Indeed,

$$\begin{aligned} \big(\tau g'(\tau)\big)^\wedge(\xi) &= \int_{\mathbb{R}}\tau g'(\tau)e^{-i2\pi\xi\tau}d\tau = \frac{1}{-i2\pi}\frac{d}{d\xi}\Big(\int_{\mathbb{R}} g'(\tau)e^{-i2\pi\xi\tau}d\tau\Big) \\ &= -\frac{1}{-i2\pi}\frac{d}{d\xi}\Big(\int_{\mathbb{R}} g(\tau)\partial_\tau\big(e^{-i2\pi\xi\tau}\big)d\tau\Big) \\ &= -\frac{d}{d\xi}\Big(\xi\int_{\mathbb{R}} g(\tau)e^{-i2\pi\xi\tau}d\tau\Big) \\ &= -\frac{d}{d\xi}\big(\xi\widehat{g}(\xi)\big) = -\widehat{g}(\xi)-\xi\big(\widehat{g}\big)'(\xi). \end{aligned}$$

Thus,

$$\begin{aligned} \partial_\eta\Big(V_x^{\mathrm{I},g'}(t,\eta)\Big) &= -i2\pi V_x^{\mathrm{I},\tau g'(\tau)}(t,\eta) \\ &= -i2\pi e^{i2\pi\varphi(t)}\int_{\mathbb{R}}\widehat{x}(\xi)\ \big(\tau g'(\tau)\big)^\wedge(\eta-\varphi'(t)-\xi)e^{i2\pi t\xi}d\xi \\ &= i2\pi V^{\mathrm{I}}(t,\eta) + i2\pi e^{i2\pi\varphi(t)} \\ &\quad \int_{\mathbb{R}}\widehat{x}(\xi)\ (\eta-\varphi'(t)-\xi)\big(\widehat{g}\big)'(\eta-\varphi'(t)-\xi)e^{i2\pi t\xi}d\xi. \end{aligned} \tag{33}$$

With the formulas (31), (32), and (33), we can obtain $Q_0(t,\eta)$ and then, $\omega_x^{\mathrm{I},2nd}(t,\eta)$.

5.2. IFE-FSST Algorithms for IF Estimation and Component Recovery and Experiments

To apply IFE-STFT or IFE-FSST, first of all we need to choose $\varphi(t)$ and $\varphi'(t)$. For the purpose of estimating the IF $\phi_k'(t)$ of the kth component $x_k(t)$ and/or recover $x_k(t)$ of a multicomponent signal $x(t)$, we should choose $\varphi(t)$ and $\varphi'(t)$ close to $\phi_k(t)$ (up to a constant) and $\phi_k'(t)$ respectively. One way is to use the ridges of the STFT. More precisely, suppose $\{t_n\}_{0\le n<N}, \{\eta_j\}_{0\le j<J}, \{\xi_m\}_{0\le m<M}$ are the sampling points of t, η, ξ respectively for STFT $V_x(t,\eta)$, FSST $R_x(t,\xi)$, and IFE-FSST $R_x^{\mathrm{I}}(t,\xi)$. Let $\widehat{\eta}_{j_n,k}, 0 \le n < N$ be the STFT ridge corresponding to $x_k(t)$ given by

$$\widehat{\eta}_{j_n,k} := \mathrm{argmax}_{\eta_j \in \mathcal{G}_{t_n,k}}\{|V_x(t_n,\eta_j)|\}, \tag{34}$$

for each n, $0 \le n < N$, where for each n, $\mathcal{G}_{t_n,k}$ is an interval containing $\phi_k'(t_n)$ (with convention: $\phi_0(t) \equiv 0$) at the time instant t_n, and $\mathcal{G}_{t_n,k}, 0 \le k \le K$ form a disjoint union of $\{\eta : |V_x(t_n,\eta)| > \gamma\}$, namely for each t_n,

$$\{\eta : |V_x(t_n,\eta)| > \gamma\} = \cup_{k=0}^{K}\mathcal{G}_{t_n,k}.$$

See more details on $\mathcal{G}_{t,k}$ in [37].

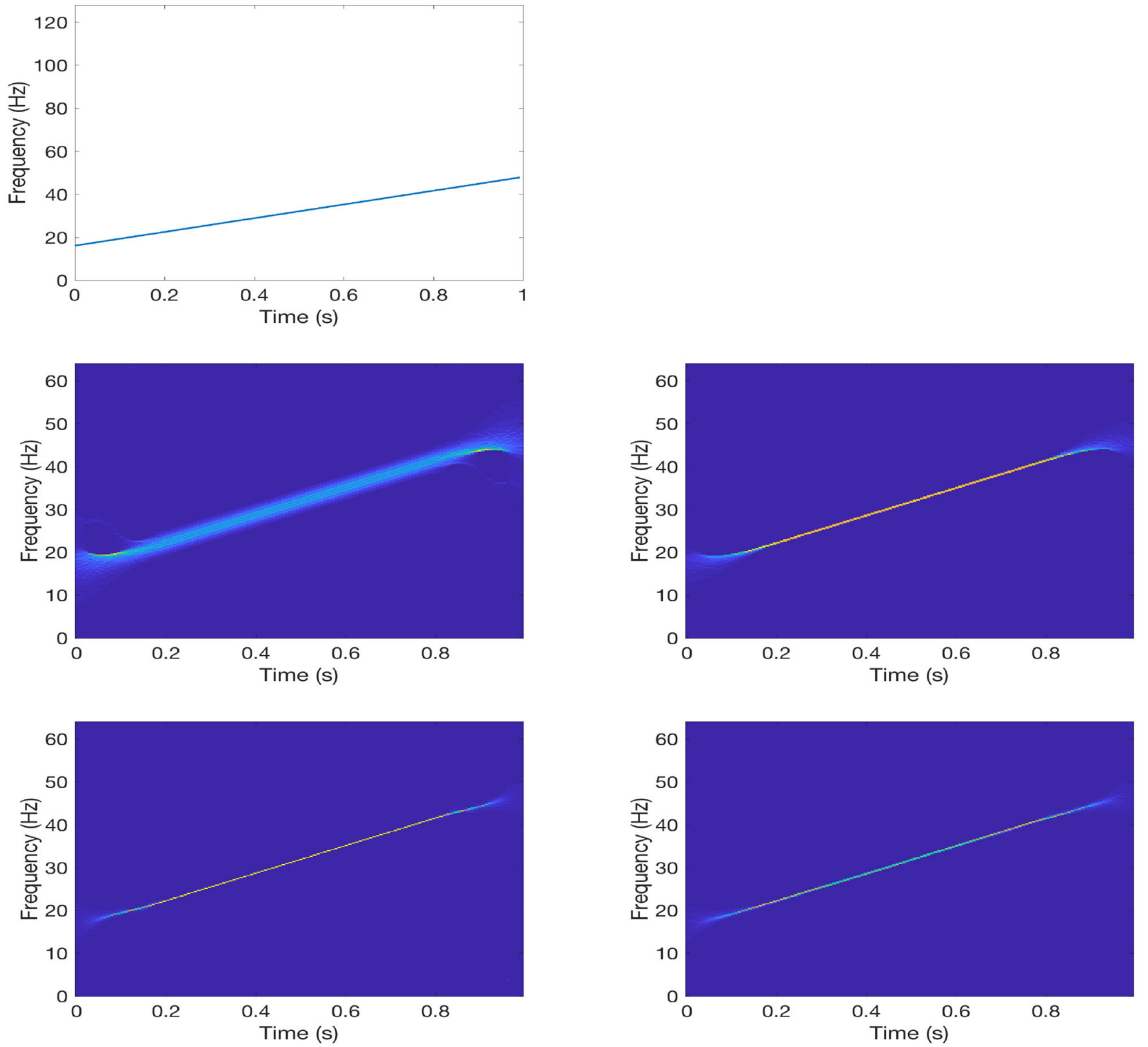

FIGURE 1 | Experiment with $x(t)$ in (43). **1st row:** IF $\phi'(t)$; **2nd row:** FSST $|R_x(t,\eta)|$ **(left)** and IFE-FSST $|R_x^{\mathrm{I}}(t,\eta)|$ **(right)**; **3rd row:** 2nd-order FSST **(left)** and 2nd-order IFE-FSST $|R_x^{\mathrm{I},2}(t,\eta)|$ **(right)**.

$\{\widehat{\eta}_{j_n,k}\}_{n=0}^{N-1}$ is called a ridge of the STFT plane or a ridge of the spectrogram $|V_x(t,\eta)|$. It provides an approximation to $\phi_k'(t_n), 0 \le n < N$ [see [36, 37, 45]]. Thus, we can use

$$\varphi'(t_n) = \widehat{\eta}_{j_n,k}, \ \varphi(t_n) = \sum_{\ell=0}^{n-1} \widehat{\eta}_{j_\ell,k} \triangle t_\ell, \ 0 \le n < N \tag{35}$$

as discrete $\varphi'(t)$ and $\varphi(t)$ to define IFE-STFT and IFE-FSST, where $\triangle t_\ell = t_\ell - t_{\ell-1}$.

To recover a component by either FSST or IFE-FSST, we need an estimate $\mathrm{IF}_k(t)$ for $\phi_k'(t)$ so that (10) or (24)/(25) can be applied. One way is to use the ridges of FSST and IFE-FSST to approximate $\phi_k'(t_n)$. More precisely, let $\widehat{\xi}_{m_n,k}, 0 \le n < N$ be the FSST ridge defined similarly to the STFT ridge in (34):

$$\widehat{\xi}_{m_n,k} := \mathrm{argmax}_{\xi_m \in \mathcal{G}_{t_n,k}} \{|R_x(t_n, \xi_m)|\}, \quad 0 \le n < N. \tag{36}$$

Then Equation (10) becomes

$$x_k(t_n) \approx x_k^{\mathrm{rec}}(t_n) := \frac{1}{g(0)} \sum_{\{m:\ |m-m_n|<M_0\}} R_x(t_n, \xi_m) \triangle \xi_m, \quad 0 \le n < N, \tag{37}$$

for some $M_0 \in \mathbb{N}$, where $\triangle \xi_m = \xi_m - \xi_{m-1}$.

Similarly, Equation (24) implies that $x_k(t)$ can be recovery from (discrete) IFE-FSST:

$$x_k(t_n) \approx x_k^{\mathrm{I,rec}}(t_n) := \frac{e^{-i2\pi\eta_0 t_n}}{g(0)} \sum_{\{m:\ |m-m_n^{\mathrm{I}}|<M_0\}} R_x^{\mathrm{I}}(t_n, \xi_m) \triangle \xi_m, \quad 0 \le n < N, \tag{38}$$

where $m_n^{\mathrm{I}}, 0 \le n < N$ are the indices for IFE-FSST ridge defined as (36) with $R_x(t_n, \xi_m)$ replaced by $R_x^{\mathrm{I}}(t_n, \xi_m)$:

$$\widehat{\xi}_{m_n^{\mathrm{I}},k} := \mathrm{argmax}_{\xi_m \in \mathcal{G}_{t_n,k}} \{|R_x^{\mathrm{I}}(t_n, \xi_m)|\}, \quad 0 \le n < N. \tag{39}$$

For real-valued $x_k(t)$ and $g(t)$, the recovery formulas (37) and (38) are respectively

$$x_k(t_n) \approx x_k^{\mathrm{rec}}(t_n) := \frac{2}{g(0)} \mathrm{Re}\Big(\sum_{\{m:\ |m-m_n|<M_0\}} R_x(t_n, \xi_m) \triangle \xi_m \Big), \quad 0 \le n < N, \tag{40}$$

and

$$x_k(t_n) \approx x_k^{\mathrm{I,rec}}(t_n) \tag{41}$$

$$:= \frac{2}{g(0)} \mathrm{Re}\Big(e^{-i2\pi\eta_0 t_n} \sum_{\{m:\ |m-m_n^{\mathrm{I}}|<M_0\}} R_x^{\mathrm{I}}(t_n, \xi_m) \triangle \xi_m \Big), \quad 0 \le n < N. \tag{42}$$

To summarize, we have the following algorithm to estimate IF $\phi_k'(t)$ and recover $x_k(t)$ by IFE-FSST.

Algorithm 1. (IFE-FSST algorithm for IF estimation and component recovery) *Let $x(t)$ be a signal of the form (1). To estimate $\phi_k'(t)$ and recover $x_k(t)$ by IFE-FSST, do the following.*

Step 1. *Obtain the STFT ridge $\widehat{\eta}_{j_n,k}, 0 \le n < N$ by (34) and $\varphi'(t_n), \varphi(t_n), 0 \le n < N$ by (35).*
Step 2. *Calculate IFE-FSST with φ', φ obtained in Step 1. The ridge $\widehat{\xi}_{m_n^{\mathrm{I}},k}, 0 \le n < N$ defined by (39) is an estimate of $\phi_k'(t)$ and $x_k^{\mathrm{I,rec}}(t)$ in (38) is an approximation to $x_k(t)$.*

We can use **Algorithm 1** to recover each component $x_k(t)$ one by one. We can also apply **Algorithm 1** to the remainder $x(t) - x_k^{\mathrm{I,rec}}(t)$ to recover another component after $x_k(t)$ is recovered; and we can repeat this procedure. The procedure of this iterative method is described as follows.

Algorithm 2. (Iterative IFE-FSST algorithm for IF estimation and component recovery) *Let $x(t)$ be a signal of the form (1).*

Step 1. *Apply **Algorithm 1** to obtain $x_1^{\mathrm{I,rec}}(t)$.*
Step 2. *Let $y_1 = x - x_1^{\mathrm{I,rec}}$. Apply **Algorithm 1** to y_1 to obtain $x_2^{\mathrm{I,rec}}(t)$.*
Step 3. *Let $y_2 = x - x_1^{\mathrm{I,rec}} - x_2^{\mathrm{I,rec}}$. Apply **Algorithm 1** to y_2 to obtain $x_3^{\mathrm{I,rec}}(t)$. Repeat this process to obtain $x_4^{\mathrm{I,rec}}(t), \cdots$, and finally $x_K^{\mathrm{I,rec}}(t)$.*

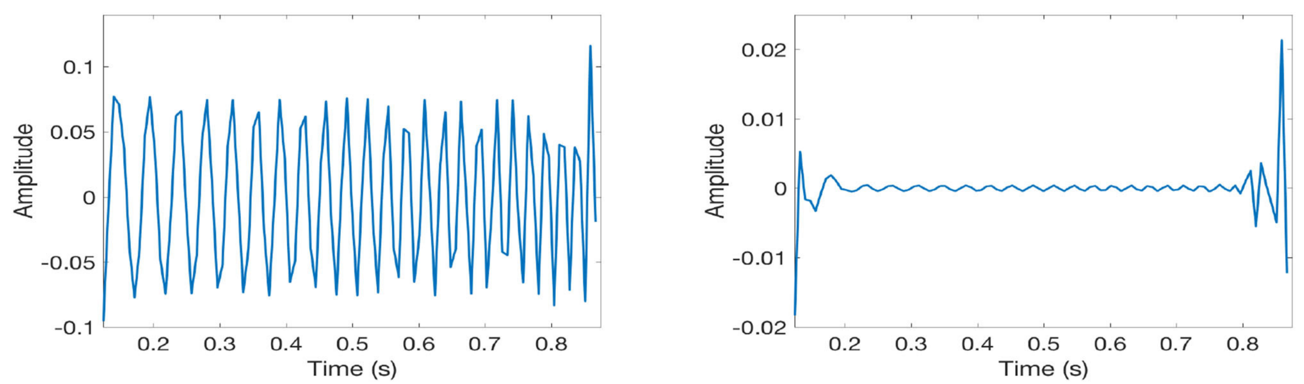

FIGURE 2 | Recovery errors for $x(t)$ given in (43) on [0.125, 0.875] by FSST **(left)** and IFE-FSST **(right)**.

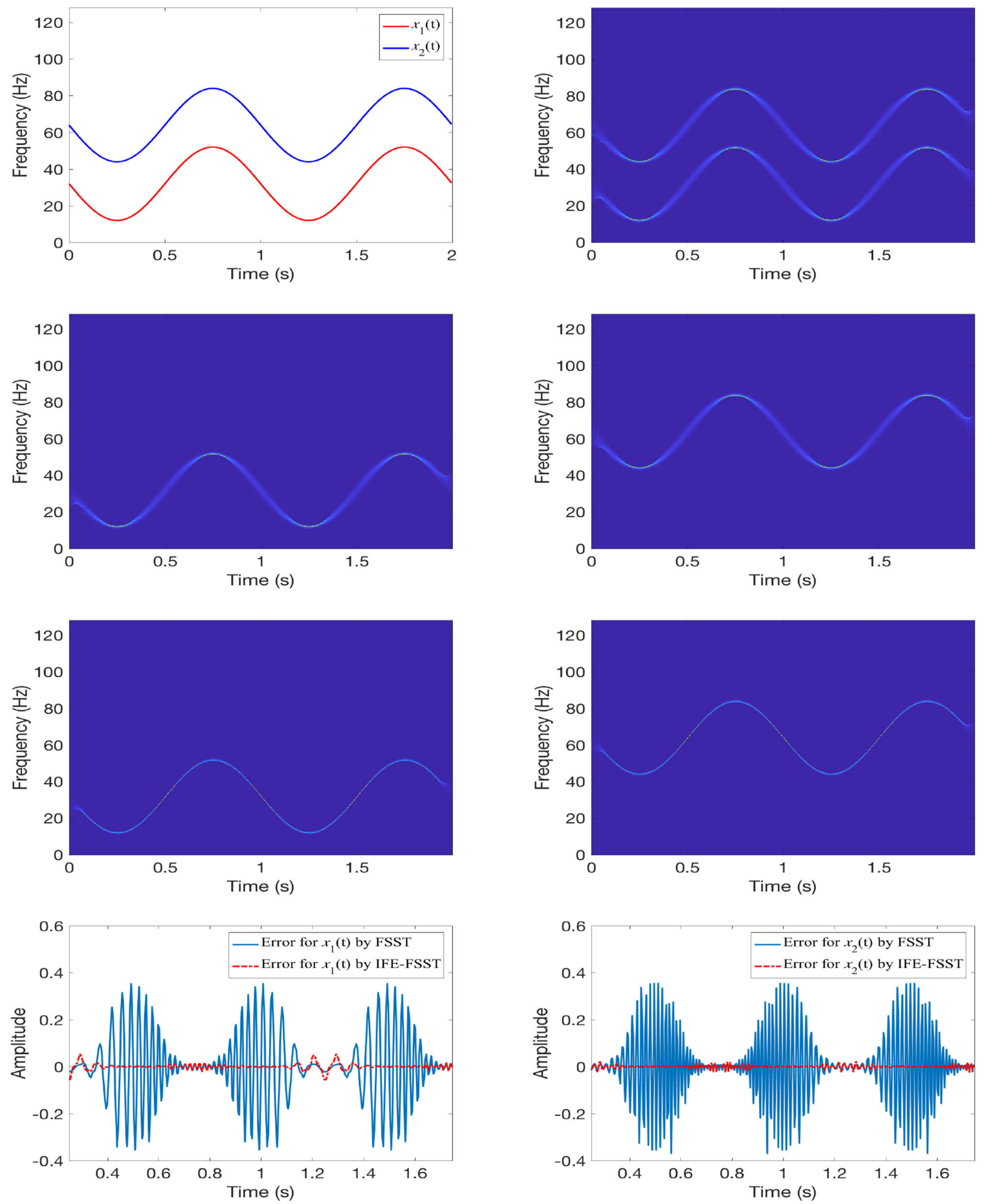

FIGURE 3 | Experiment with $x(t)$ in (44). **1st row:** IFs $\phi_1'(t), \phi_2'(t)$ **(left)** and FSST $|R_x(t, \eta)|$ **(right)**; **2nd row:** FSST for $x_1(t)$ **(left)** and FSST for $x_2(t)$ **(right)**; **3rd row:** IFE-FSST for $x_1(t)$ **(left)** and IFE-FSST for $x_2(t)$ **(right)**. **4th row:** recovery errors on $[0.125, 1.875)$ by FSST and IFE-FSST for $x_1(t)$ **(left)** and $x_2(t)$ **(right)**.

Step 4. *Apply* ***Algorithm 1*** *to* $x - \sum_{k=2}^{K} x_k^{\mathrm{I,rec}}$ *to recover* $x_1(t)$. *Let* $\widetilde{x}_1^{\mathrm{I,rec}}(t)$ *be the recovered* $x_1(t)$. *Then Apply* ***Algorithm 1*** *to* $x - \widetilde{x}_1^{\mathrm{I,rec}}(t) - \sum_{k=3}^{K} x_k^{\mathrm{I,rec}}$ *to recover* $x_2(t)$. *Let* $\widetilde{x}_2^{\mathrm{I,rec}}(t)$ *be the recovered* $x_2(t)$. *Obtain* $\widetilde{x}_3^{\mathrm{I,rec}}(t)$ *by applying* ***Algorithm 1*** *to* $x - \widetilde{x}_1^{\mathrm{I,rec}}(t) - \widetilde{x}_2^{\mathrm{I,rec}}(t) - \sum_{k=4}^{K} x_k^{\mathrm{I,rec}}$. *Repeat this process to obtain* $\widetilde{x}_4^{\mathrm{I,rec}}(t), \cdots$, *and finally* $\widetilde{x}_K^{\mathrm{I,rec}}(t)$.

We can repeat the procedure in Step 4 of **Algorithm 2**. That is why we call **Algorithm 2** an iterative algorithm.

Next we consider two examples. We let

$$g(t) = \frac{1}{\sigma\sqrt{2\pi}} e^{-\frac{t^2}{2\sigma^2}},$$

be the window function, where $\sigma > 0$. First we consider a mono-component signal

$$x(t) = \cos\big(2\pi(\phi(t)\big) = \cos\big(2\pi(16t + 16t^2)\big),\ t \in [0,1), \quad (43)$$

where $x(t)$ is uniformly sampled with sample points $t_n = n\triangle t, 0 \le n < N = 128, \triangle t = \frac{1}{128}$. The IF of $x(t)$ is $\phi'(t) = 16 + 32t$ and it is shown in the 1st row of **Figure 1**. The FSST and IFE-FSST of $x(t)$ are provided in the 2nd row; and the 2nd-order FSST and IFE-FSST are shown in the 3rd row. In this example we let $\sigma = \frac{1}{16}$. As mentioned above, discrete $\varphi'(t)$ and $\varphi(t)$ defined by (35) are used to define IFE-STFT and the 2nd-order IFE-STFT. Obviously IFE-FSST provides a much sharper time-frequency representation of $x(t)$ than FSST. Both the 2nd-order FSST and the 2nd-order IFE-FSST as well give sharp time-frequency representations of $x(t)$.

For a mono-component signal $x(t)$ as given by (43), since $x(t)$ can be recovered from FSST or IFE-FSST as shown in (8) and (22) respectively, theoretically, either (40) or (41) gives high accurate approximation to $x(t)$ as long as M_0 is large enough. We choose a small M_0 so that the recovery errors with it show how sharp the time-frequency representations with FSST and IFE-FSST are. Here and below we set $M_0 = 8$.

In **Figure 2**, we provide the recovery errors $x^{\mathrm{rec}}(t_n) - x(t_n)$, $x^{\mathrm{I,rec}}(t_n) - x(t_n)$ for $x(t)$ by FSST and IFE-FSST, where $x^{\mathrm{rec}}(t_n)$ and $x^{\mathrm{I,rec}}(t_n)$ are given by (40) and (41) respectively with $M_0 = 8$. Here, we show the error on $[0.125, 0.875)$ only to ignore the boundary effect. Obviously, IFE-FSST provides a much sharper time-frequency representation than FSST.

Next we consider a two-component signal given by

$$x(t) = x_1(t) + x_2(t),\ x_1(t) = \cos\Big(2\pi\Big(32t + \frac{10}{\pi}\cos(2\pi t)\Big)\Big),$$
$$x_2(t) = \cos\Big(2\pi\Big(64t + \frac{10}{\pi}\cos(2\pi t)\Big)\Big), \quad (44)$$

where $t \in [0,2)$, and $x(t)$ is uniformly sampled with sample points $t_n = n\triangle t, 0 \le n < N = 512, \triangle t = \frac{1}{256}$. Thus, IFs of $x_1(t), x_2(t)$ are $\phi_1'(t) = 32 - 20\sin(2\pi t), \phi_2'(t) = 64 - 20\sin(2\pi t)$, which are shown on the top-left panel of **Figure 3**. In this example we let $\sigma = \frac{1}{32}$ for the window function.

To this two-component signal, we apply **Algorithm 2** to obtain $\widetilde{x}_1^{\mathrm{I,rec}}(t)$ and $\widetilde{x}_2^{\mathrm{I,rec}}(t)$. In the 3rd row of **Figure 3** we show the IFE-FSSTs of $\widetilde{x}_1^{\mathrm{I,rec}}(t)$ and $\widetilde{x}_2^{\mathrm{I,rec}}(t)$. The FSST of $x(t)$ is provided in the top-right panel of **Figure 3**. Of course, we can also apply iterative method to FSST to recover components one by one. Namely, we apply FSST to obtain $x_1^{\mathrm{rec}}(t)$, then apply FSST to $x(t) - x_1^{\mathrm{rec}}(t)$ to obtain $x_2^{\mathrm{rec}}(t)$. After that we apply FSST to $x(t) - x_2^{\mathrm{rec}}(t)$ to obtain $\widetilde{x}_1^{\mathrm{rec}}(t)$, and finally to obtain $\widetilde{x}_2^{\mathrm{rec}}(t)$ by applying FSST to $x(t) - \widetilde{x}_1^{\mathrm{rec}}(t)$.

The 2nd row of **Figure 3** shows the FSSTs of $\widetilde{x}_1^{\mathrm{rec}}(t)$ and $\widetilde{x}_2^{\mathrm{rec}}(t)$. Comparing the FSST of x in the top-right panel with the individual FSSTs in the 2nd row, we see there is not much improvement of the time-frequency representation of FSST of x after we apply the iterative component recovery procedure.

In the 4th row of **Figure 3**, we provide the recovery errors for $x_1(t), x_2(t)$ by FSST and IFE-FSST. Here, we show the error on $[0.125, 1.875)$. From **Figure 3**, we see IFE-FSST provides a much sharper time-frequency representation for $x(t)$. We also consider FSST and IFE-FSST of two-component $x(t)$ in the noisy environment and our experiments show that IFE-FSST provides a sharp time-frequency representation in the noisy environment. In addition, we consider the 2nd-order IFE-FSST for component recovery. It does not provide much improvement than IFE-FSST. This may be due to that the results from IFE-FSST are hard to improve. Due to that only 15 pictures are allowed to be included in a article in this journal, we do not present these results here.

DATA AVAILABILITY STATEMENT

The original contributions presented in the study are included in the article/supplementary material, further inquiries can be directed to the corresponding author/s.

ETHICS STATEMENT

This article was approved by AFRL for public release on 03 Dec. 2021, Case Number: AFRL-2021-4285, Distribution unlimited.

AUTHOR CONTRIBUTIONS

All authors listed have made a substantial, direct, and intellectual contribution to the work and approved it for publication.

FUNDING

This work was supported in part by Simons Foundation (Grant No. 353185) and the 2020 Air Force Summer Faculty Fellowship Program (SFFP).

REFERENCES

1. Daubechies I, Lu J, Wu H-T. Synchrosqueezed wavelet transforms: an empirical mode decomposition-like tool. *Appl Comput Harmon Anal*. (2011) 30:243–61. doi: 10.1016/j.acha.2010.08.002
2. Huang NE, Shen Z, Long SR, Wu ML, Shih HH, Zheng Q, et al. The empirical mode decomposition and Hilbert spectrum for nonlinear and nonstationary time series analysis. *Proc R Soc Lond A*. (1998) 454:903–95. doi: 10.1098/rspa.1998.0193
3. Wu Z, Huang NE. Ensemble empirical mode decomposition: a noise-assisted data analysis method. *Adv Adapt Data Anal*. (2009) 1:1–41. doi: 10.1142/S1793536909000047
4. Flandrin P, Rilling G, Goncalves P. Empirical mode decomposition as a filter bank. *IEEE Signal Proc Lett*. (2004) 11:112–4. doi: 10.1109/LSP.2003.821662
5. Li L, Ji H. Signal feature extraction based on improved EMD method. *Measurement*. (2009) 42:796–803. doi: 10.1016/j.measurement.2009.01.001
6. Rilling G, Flandrin P. One or two frequencies? The empirical mode decomposition answers. *IEEE Trans Signal Proc*. (2008) 56:85–95. doi: 10.1109/TSP.2007.906771
7. Lin L, Wang Y, Zhou HM. Iterative filtering as an alternative algorithm for empirical mode decomposition. *Adv Adapt Data Anal*. (2009) 1:543–60. doi: 10.1142/S179353690900028X
8. Xu Y, Liu B, Liu J, Riemenschneider S. Two-dimensional empirical mode decomposition by finite elements. *Proc R Soc Lond A*. (2006) 462:3081–96. doi: 10.1098/rspa.2006.1700
9. van der Walt MD. Empirical mode decomposition with shape-preserving spline interpolation. *Results Appl Math*. (2020) 5:100086. doi: 10.1016/j.rinam.2019.100086
10. Wang Y, Wei G-W, Yang SY. Iterative filtering decomposition based on local spectral evolution kernel. *J Sci Comput*. (2012) 50:629–64. doi: 10.1007/s10915-011-9496-0
11. Zheng JD, Pan HY, Liu T, Liu QY. Extreme-point weighted mode decomposition. *Signal Proc*. (2018) 42:366–74. doi: 10.1016/j.sigpro.2017.08.00
12. Cicone A, Liu JF, Zhou HM. Adaptive local iterative filtering for signal decomposition and instantaneous frequency analysis. *Appl Comput Harmon Anal*. (2016) 41:384–411. doi: 10.1016/j.acha.2016.03.001
13. Thakur G, Wu H-T. Synchrosqueezing based recovery of instantaneous frequency from nonuniform samples. *SIAM J Math Anal*. (2011) 43:2078–95. doi: 10.1137/100798818
14. Wu H-T. *Adaptive analysis of complex data sets*. Ph.D. dissertation. Princeton University Press, Princeton, NJ, United States (2012).
15. Oberlin T, Meignen S, Perrier V. The Fourier-based synchrosqueezing transform. In: *Proc. 39th Int. Conf. Acoust., Speech, Signal Proc*. (*ICASSP)*. Beijing (2014). p. 315–9. doi: 10.1109/ICASSP.2014.6853609
16. Oberlin T, Meignen S, Perrier V. Second-order synchrosqueezing transform or invertible reassignment? Towards ideal time-frequency representations. *IEEE Trans Signal Proc*. (2015) 63:1335–44. doi: 10.1109/TSP.2015.2391077
17. Oberlin T, Meignen S. The 2nd-order wavelet synchrosqueezing transform. In: *2017 IEEE International Conference on Acoustics, Speech and Signal Processing (ICASSP)*. New Orleans, LA (2017). doi: 10.1109/ICASSP.2017.7952906
18. Lu J, Alzahrani JH, Jiang QT. A second-order synchrosqueezing transform with a simple phase transformation. *Num Math Theory Methods Appl*. (2021) 14: 624–49. doi: 10.4208/nmtma.OA-2020-0077
19. Pham D-H, Meignen S. High-order synchrosqueezing transform for multicomponent signals analysis - With an application to gravitational-wave signal. *IEEE Trans Signal Proc*. (2017) 65:3168–78. doi: 10.1109/TSP.2017.2686355
20. Li L, Wang ZH, Cai HY, Jiang QT, Ji HB. Time-varying parameter-based synchrosqueezing wavelet transform with the approximation of cubic phase functions. In: *2018 14th IEEE Int'l Conference on Signal Proc. ICSP*. New Orleans, LA (2018). p. 844–8. doi: 10.1109/ICSP.2018.8652362
21. Chui CK, van der Walt MD. Signal analysis via instantaneous frequency estimation of signal components. *Int J Geomath*. (2015) 6:1–42. doi: 10.1007/s13137-015-0070-z
22. Chui CK, Lin Y-T, Wu H-T. Real-time dynamics acquisition from irregular samples - with application to anesthesia evaluation. *Anal Appl*. (2016) 14:537–90. doi: 10.1142/S0219530515500165
23. Daubechies I, Wang Y, Wu H-T. ConceFT: concentration of frequency and time via a multitapered synchrosqueezed transform. *Philos Trans R Soc A*. (2016) 374:20150193. doi: 10.1098/rsta.2015.0193
24. Yang HZ. Synchrosqueezed wave packet transforms and diffeomorphism based spectral analysis for 1D general mode decompositions. *Appl Comput Harmon Anal*. (2015) 39:33–66. doi: 10.1016/j.acha.2014.08.004
25. Yang HZ, Ying LX. Synchrosqueezed curvelet transform for two-dimensional mode decomposition. *SIAM J. Math Anal*. (2014) 3:2052–83. doi: 10.1137/130939912
26. Sheu Y-L, Hsu L-Y, Chou P-T, Wu H-T. Entropy-based time-varying window width selection for nonlinear-type time-frequency analysis. *Int J Data Sci Anal*. (2017) 3:231–45. doi: 10.1007/s41060-017-0053-2
27. Berrian AJ, Saito N. Adaptive synchrosqueezing based on a quilted short-time Fourier transform. *arXiv [Preprint] arXiv*:1707.03138v5. (2017). doi: 10.1117/12.2271186
28. Li L, Cai HY, Han HX, Jiang QT, Ji HB. Adaptive short-time Fourier transform and synchrosqueezing transform for non-stationary signal separation. *Signal Proc*. (2020) 166:107231. doi: 10.1016/j.sigpro.2019.07.024
29. Li L, Cai HY, Jiang QT. Adaptive synchrosqueezing transform with a time-varying parameter for non-stationary signal separation. *Appl Comput Harmon Anal*. (2020) 49:1075–106. doi: 10.1016/j.acha.2019.06.002
30. Cai HY, Jiang QT, Li L, Suter BW. Analysis of adaptive short-time Fourier transform-based synchrosqueezing transform. *Anal Appl*. (2021) 19:71–105. doi: 10.1142/S0219530520400047
31. Lu J, Jiang QT, Li L. Analysis of adaptive synchrosqueezing transform with a time-varying parameter. *Adv Comput Math*. (2020) 46:72. doi: 10.1007/s10444-020-09814-x
32. Li C, Liang M. Time frequency signal analysis for gearbox fault diagnosis using a generalized synchrosqueezing transform. *Mech Syst Signal Proc*. (2012) 26:205–17. doi: 10.1016/j.ymssp.2011.07.001
33. Wang SB, Chen XF, Selesnick IW, Guo YJ, Tong CW, Zhang XW. Matching synchrosqueezing transform: a useful tool for characterizing signals with fast varying instantaneous frequency and application to machine fault diagnosis. *Mech Syst Signal Proc*. (2018) 100:242–88. doi: 10.1016/j.ymssp.2017.07.009
34. Wu H-T. Current state of nonlinear-type time-frequency analysis and applications to high-frequency biomedical signals. *Curr Opin Syst Biol*. (2020) 23:8–21. doi: 10.1016/j.coisb.2020.07.013
35. Chui CK, Mhaskar HN. Signal decomposition and analysis via extraction of frequencies. *Appl Comput Harmon Anal*. (2016) 40:97–136. doi: 10.1016/j.acha.2015.01.003
36. Li L, Chui CK, Jiang QT. Direct signal separation via extraction of local frequencies with adaptive time-varying parameter. *arXiv [Preprint] arXiv*:2010.01866. (2020).
37. Chui CK, Jiang QT, Li L, Lu J. Analysis of an adaptive short-time Fourier transform-based multicomponent signal separation method derived from linear chirp local approximation. *J Comput Appl Math*. (2021) 396:113607. doi: 10.1016/j.cam.2021.113607
38. Chui CK, Han NN. Wavelet thresholding for recovery of active sub-signals of a composite signal from its discrete samples. *Appl Comput Harmon Anal*. (2021) 52:1–24. doi: 10.1016/j.acha.2020.11.003
39. Chui CK, Jiang QT, Li L, Lu J. Signal separation based on adaptive continuous wavelet-like transform and analysis. *Appl Comput Harmon Anal*. (2021) 53:151–79. doi: 10.1016/j.acha.2020.12.003
40. Chui CK, Mhaskar HN, van der Walt MD. Data-driven atomic decomposition via frequency extraction of intrinsic mode functions. *Int J Geomath*. (2016) 7:117–46. doi: 10.1007/s13137-015-0079-3
41. Li C, Liang M. A generalized synchrosqueezing transform for enhancing signal time-frequency representation. *Signal Proc*. (2012) 92:2264–74. doi: 10.1016/j.sigpro.2012.02.019
42. Meignen S, Pham D-H, McLaughlin S. On demodulation, ridge detection, and synchrosqueezing for multicomponent signals. *IEEE Trans Signal Proc*. (2017) 65:2093–103. doi: 10.1109/TSP.2017.2656838

43. Wang SB, Chen XF, Cai GG, Chen BQ, Li X, He ZJ. Matching demodulation transform and synchrosqueezing in time-frequency analysis. *IEEE Trans Signal Proc*. (2014) 62:69–84. doi: 10.1109/TSP.2013.2276393
44. Jiang QT, Suter BW. Instantaneous frequency estimation based on synchrosqueezing wavelet transform. *Signal Proc*. (2017) 138:167–81. doi: 10.1016/j.sigpro.2017.03.007
45. Stankovic L, Dakovic M, Ivanovic V. Performance of spectrogram as IF estimator. *Electron Lett*. (2001) 37:797–9. doi: 10.1049/el:20010517

Conflict of Interest: The authors declare that the research was conducted in the absence of any commercial or financial relationships that could be construed as a potential conflict of interest.

Publisher's Note: All claims expressed in this article are solely those of the authors and do not necessarily represent those of their affiliated organizations, or those of the publisher, the editors and the reviewers. Any product that may be evaluated in this article, or claim that may be made by its manufacturer, is not guaranteed or endorsed by the publisher.